Available online at www.sciencedirect.com
SCIENCE DIRECT
ELSEVIER
Icarus 176 (2005) 175–183
ICARUS
www.elsevier.com/locate/icarus

Radar observations of Comet 2P/Encke during the 2003 apparition

John K. Harmon *, Michael C. Nolan

National Astronomy and Ionosphere Center, Arecibo Observatory, HC3 Box 53995, Arecibo, PR 00612, USA

Received 23 September 2004; revised 14 January 2005

Available online 24 March 2005

Abstract

The nucleus of Comet 2P/Encke was detected with the Arecibo radar during the close approach of November, 2003, making this the first comet to yield radar detections at two different apparitions. Although the measured radar cross section of 1.0 km^2 was close to that obtained in 1980, the Doppler bandwidth was nearly four times larger. Most of this bandwidth difference can simply be attributed to a different observing aspect relative to the spin axis proposed by Sekanina [1988, Astron. J. 95, 911] and Festou and Barale [2000, Astron. J. 119, 3119]. Comparison of the 2003 Doppler bandwidth with infrared-based size estimates supports an 11-h dominant rotation period and excludes slower 15- and 22-h periods that have also been suggested. If one assumes a short-axis-mode rotation with an 11-h period, then the Doppler bandwidth indicates that the nucleus is an oblong object with a long-axis dimension of 9 km. The estimated radar albedo of 0.05 is similar to that measured for C/IRAS–Araki–Alcock, providing further evidence that comet nuclei have relatively low surface densities of $\sim$0.5–1.0 g cm^{-3}. No broadband echo component was detected from large coma grains despite predictions, based on optical/infrared models, that such a component might be detectable.

Keywords: Comets; Radar; Surfaces, comets

1. Introduction

Comet Encke is among the most famous and intensively studied of all the comets (Sekanina, 1991). It was also the first comet to be detected with radar (Kamoun et al., 1982a,1982b; Kamoun, 1983). The 1980 Arecibo radar observations, which were centered around the November close approach ($\Delta = 0.32$ AU), revealed a weak (6 standard deviations) Doppler spike from the nucleus after several days of integration (Kamoun et al., 1982b). This detection was made using an unmodulated CW (continuous wave) transmission, which yields an echo Doppler spectrum but no delay resolution. Although this observing mode gives no direct size information, Encke's measured radar cross section of 1.1 ± 0.7 km^2 was consistent with a nucleus size of a few kilometers if one assumed some plausible radar albedo. The other radar parameters derived from the 1980 detection were a rotational (Doppler) bandwidth of 6 ± 3 Hz and a mean Doppler offset (relative to the prediction ephemeris) of +7.5 Hz. The Doppler bandwidth estimate was based on the bandwidth of the smoothing filter that optimized the detection, and only in that sense can the 1980 detection be said to have been resolved in frequency.

In the years since that first Encke detection, eight more comets have been detected (all in CW mode) with the Arecibo and/or Goldstone radars. Of the eight, five showed a narrow-band Doppler echo from the nucleus similar to that seen for Encke. In addition, a broad-band echo component from large (>cm-size) coma grains was detected for five of the eight comets, two of which (C/IRAS–Araki–Alcock and C/Hyakutake) also showed a nucleus echo. For reviews of these comet radar results, and more details on comet radar techniques and interpretation, see Harmon et al. (1999) and Harmon et al. (2004).

Comet Encke, despite its short orbital period, would not return to radar-detectable range until November, 2003. The 2003 apparition offered the best Encke radar opportunity that

* Corresponding author. Fax: +1-787-878-1861.
E-mail address: harmon@naic.edu (J.K. Harmon).

0019-1035/$ – see front matter
doi:10.1016/j.icarus.2005.01.012

we would have for many years. It would also be our first chance to make a second detection of the same comet at a different apparition and, in this case, from a very different directional aspect. The closer approach distance ($\Delta = 0.26$ AU) in 2003, combined with the improved sensitivity of the upgraded Arecibo radar, ensured a much stronger detection than in 1980. There was even considered to be some chance of obtaining crude delay-Doppler images for direct estimation of nucleus size and rotation. However, radar detectability decreases rapidly ($\sim\Delta^{-4}$) with distance Δ, making detailed imaging unfeasible at distances much greater than 0.10 AU (Harmon et al., 1999, 2004). This, combined with the rarity of close comet approaches, is the main reason no comet nucleus has yet been imaged with radar. Nevertheless, we did attempt a 2-μs delay-Doppler observation on November 22. Our failure to obtain a detection from this observation was apparently due to insufficient echo strength, a problem that was compounded by the echo's unexpectedly large Doppler bandwidth and the loss of a transmitter klystron (which reduced the transmitted power to less than half the nominal 900 KW). We abandoned further delay-Doppler attempts and switched to CW mode for the remainder of the observations, obtaining good detections of the nucleus on each of the subsequent three days (November 23–25).

The measured Doppler spectra from these observations yielded accurate radar cross section and bandwidth estimates for the nucleus. The bandwidth, when compared with the 1980 value, places a strong constraint on the spin axis (Section 3). It can also be used to constrain the nucleus size and rotation period when compared with other observations (Section 4). Although we considered there to be a reasonable likelihood of a grain-coma detection for this comet, no such component was detected. We have used this null detection to place an upper limit on the abundance of large grains being ejected by Encke a month before perihelion (Section 5).

2. Observations and results

The radar detections were made on November 23, 24, and 25, 2003 with the S-band radar on the Arecibo 305-m telescope. This radar operated at a frequency of 2380 MHz (wavelength $\lambda = 12.6$ cm), the same as for the 1980 detection. The observing times and measured radar parameters are listed in Table 1. The comet's geocentric distance Δ ranged from 0.275 AU (November 23) to 0.284 AU (November 25) and its mean heliocentric distance was 0.876 AU. The start date was postponed to several days after the November 16 ($\Delta = 0.261$ AU) close approach owing to a klystron failure (in a dual-klystron system) and other telescope problems. The system was reconfigured for single-klystron operation, allowing us to transmit at a reduced power of 400 KW. We transmitted a circularly polarized CW (unmodulated) wave and received both orthogonal circular polarizations. (For the received polarization senses we will adopt the usual notation of "OC" for the "opposite circular" sense and "SC" for the "same circular" sense, relative to the transmitted sense.) Between 13 and 15 observing runs (transmit/receive cycles) were conducted over a span of 2.1–2.6 h on a given day, giving a daily receive integration time of 1.0–1.2 h and a total integration time for the three days of 3.4 h.

Table 1
Radar cross sections and polarization ratios

Date(s) (UT)	σ_{oc} (km^2)	μ_c
2003 November 23.81	$0.74 \pm 0.16(0.06)$[a]	0.16 ± 0.08
2003 November 24.82	$0.76 \pm 0.16(0.05)$[a]	0.21 ± 0.07
2003 November 25.80	$1.05 \pm 0.22(0.08)$[a]	0.22 ± 0.07
2003 November 23–25	$0.84 \pm 0.17(0.04)$[a]	0.21 ± 0.04

Note. All errors are 1 standard deviation.
[a] The quoted error in σ_{oc} represents the quadratic sum of the random noise error and a 20% allowance for systematic calibration error. Also given (in parentheses) is the random error alone.

Telescope pointing and receive-time Doppler compensation were done using a topocentric observing ephemeris provided by Jon D. Giorgini of the Jet Propulsion Laboratory (JPL). This ephemeris was generated on November 14 using the JPL K035/18 orbit solution for Encke. The changing Doppler offset of the echo was removed by continuously drifting the receiver local oscillator according to this ephemeris, so that zero frequency in our Doppler spectra corresponds to the nominal center frequency of the nucleus as predicted by the ephemeris. No a posteriori adjustment has been done to remove any residual Doppler offset. As it turned out, the nucleus echoes on each of the three days came in precisely on the nominal frequency with no evidence of offset or drift, which attests to the accuracy of the JPL ephemeris. (The a priori Doppler accuracy of the JPL K035/18 ephemeris was estimated to be 0.17 Hz, which represents a 3-standard-deviations formal error and does not include possible systematic error from outgassing events or other changes in nongravitational acceleration.) For astrometric reference purposes (Yeomans et al., 1992; Ostro et al., 2002) we quote the following JPL-K035/18 ephemeris predictions for the Arecibo topocentric delay and Doppler of the Encke nucleus at a reference time of 19:00:00 UT on the three observing days: (274.275857 s, −112487.565 Hz) on November 23; (278.682729 s, −128479.125 Hz) on November 24; and (283.651734 s, −144166.475 Hz) on November 25.

An echo from the Encke nucleus was clearly visible on each of the three days. This can be seen from Fig. 1, which shows the daily-average echo power spectra in the OC and SC polarizations. In Fig. 2 we show the spectra averaged over all three days. For both figures, the spectra were obtained from 1-Hz-resolution raw spectra which were then Hanning smoothed (i.e., 3-point smoothed with weights of 0.25, 0.50, 0.25). Smoothing the 3-day-average OC spectrum with a fitted model spectrum (see below) gives a matched-filtered peak amplitude (or signal-to-noise ratio SNR) of 29 noise standard deviations, or about 5 times the SNR of the 1980 detection. The corresponding SNR for our

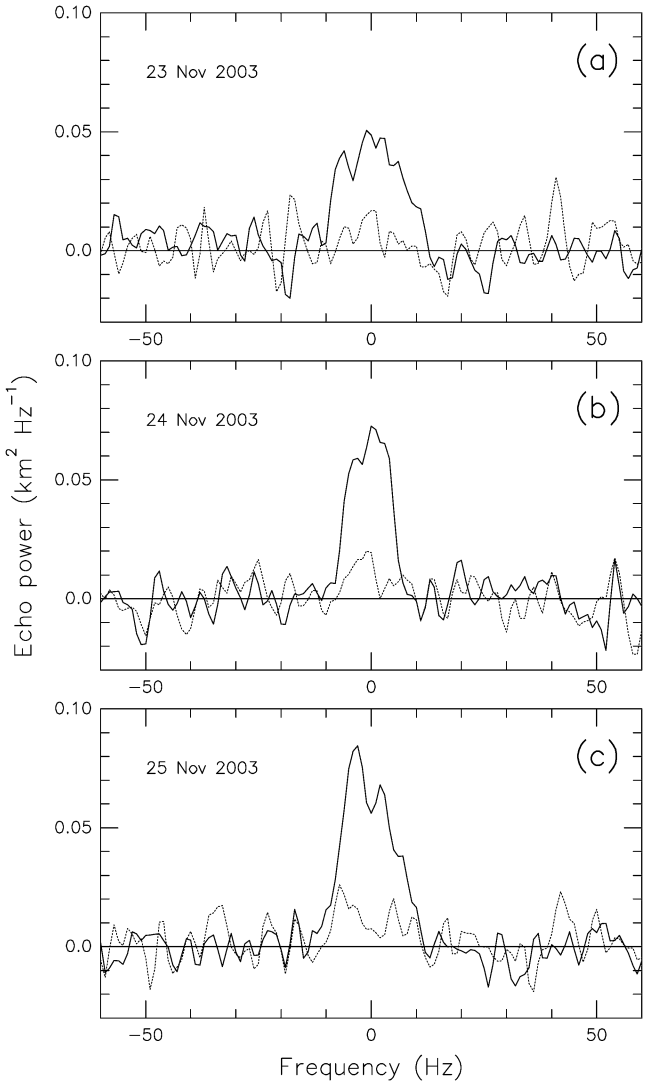

Fig. 1. Echo spectra in the OC (solid line) and SC (dotted line) polarizations for (a) November 23, (b) November 24, and (c) November 25, 2003. All spectra are Hanning smoothed from the 1-Hz-resolution raw spectra.

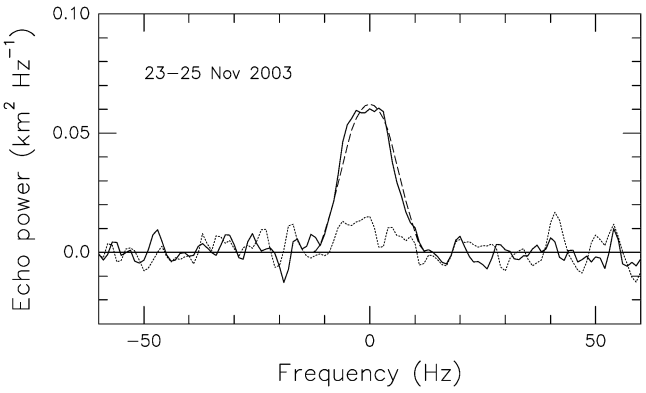

Fig. 2. Echo spectra in the OC (solid line) and SC (dotted line) polarizations, averaged over all three days. Also shown is the fitted spectrum (dashed line) used to obtain the $B = 22.9 \pm 1.4$ Hz estimate for the Doppler bandwidth.

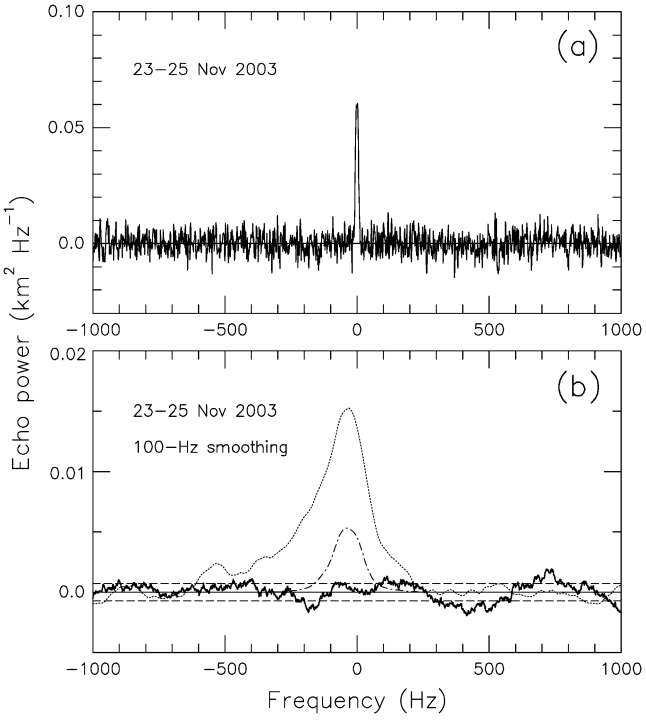

Fig. 3. (a) The 3-day average OC spectrum from Fig. 2 plotted on a wider frequency scale. (b) The 3-day average OC spectrum (heavy solid line) after notching out the nucleus echo and then smoothing with a 100-Hz boxcar filter. Also shown are the ±1 standard deviation levels (horizontal dashed lines) and the 100-Hz-smoothed coma echoes from Comets C/2001 A2 (LINEAR) (dotted line) and C/IRAS–Araki–Alcock (dot-dashed line).

SC echo is 5 standard deviations. The fact that the OC echo is much the stronger of the two polarizations is an attribute that Encke shares with all of the other radar-detected comet nuclei (Harmon et al., 1999, 2004), the terrestrial planets, and most asteroids. A dominant OC echo is a characteristic of conventional surface backscatter, the OC polarization being the expected sense for specular reflection.

We found no evidence for a grain-coma echo, which would have been easily distinguished from the narrow nucleus echo by the large (hundreds of Hz) Doppler spread associated with an ensemble of moving grains. This null result is apparent from the spectra in Fig. 3; here Fig. 3a shows the 3-day OC spectrum of Fig. 2 on a wider frequency scale, while Fig. 3b shows the 3-day OC spectrum smoothed with a 100-Hz boxcar after first notching out the nucleus echo.

Radar cross sections σ_{oc} and σ_{sc} have been computed by integrating under the OC and SC nucleus echo features. In Table 1 we list σ_{oc} and the circular polarization ratio $\mu_c = \sigma_{sc}/\sigma_{oc}$ estimated from the spectra in Figs. 1 and 2. Our mean σ_{oc} of 0.84 ± 0.17 km^2 agrees well with the $\sigma_{oc} = 1.1 \pm 0.7$ km^2 reported from the 1980 observations. Although the difference between the 1980 and 2003 σ_{oc} values is not significant, the fact that the 1980 value is the larger of the two would be consistent with the more "pole-on" observing geometry that we have deduced for the 1980 apparition (Section 3). In any case, the new result confirms Encke as having the second highest radar cross section (after C/IRAS–Araki–Alcock) of the six comet nuclei de-

tected to date (Harmon et al., 1999, 2004). This implies a moderately large nucleus for Encke, which is consistent with other data (see Section 4). The measured μ_c value is similar to the 0.1–0.2 values measured for C/IRAS–Araki–Alcock and C/Sugano–Saigusa–Fujikawa (Harmon et al., 1989, 1999) and comparable to the μ_c measured for many near-Earth asteroids (Ostro et al., 1991; Magri et al., 2001; Harmon et al., 2004; L.A.M. Benner, personal comm.). (There is no μ_c estimate for Encke from 1980 as those observations were done in OC-only mode.) The Encke μ_c value is consistent with single scattering off a surface that is not particularly rough at wavelength (decimeter) scales. On the other hand, the spectra in Figs. 1 and 2 have a rather squared-off shape similar to that of other comets and asteroids, which may be an indicator of a high degree of superwavelength-scale (blocky) roughness (Harmon et al., 1989, 1999). The squared-off appearance could also be enhanced if one is observing an oblong nucleus over a wide range of rotational phases.

That the Encke nucleus is oblong is obvious from the fact that the spectrum from November 24 is clearly narrower than the spectra from the other two days. The bandwidth variation indicates an axial ratio of at least 1.4, while other (nonradar) observations suggest an axial ratio of 2.0 or so (see Section 4). In principle, one could deduce a rotation period from changes in the shape and bandwidth of the Doppler spectrum as the oblong nucleus rotates. We compared spectra from shorter (single-run or double-run) integrations to look for intra-day changes that might warrant an attempt at a full rotation model. The second day (November 24) did show some spectral variation that may have been caused by rotation, but the detailed character of these changes and the low signal-to-noise ratios for the short-integration spectra convinced us that it would be impossible to extract a reliable rotation period from the radar data alone.

Given the relatively short rotation period currently preferred for this comet (Section 3), we deduce that the 3-day-average spectrum (Fig. 2) should represent an average over the full range of rotational orientations. Hence, the total bandwidth of the spectrum in Fig. 2 is likely to be a good estimate of the maximum bandwidth. To make an estimate of this bandwidth in the presence of noise, we fit the spectrum with a model spectrum based on a prolate spheroid (2:1 axial ratio) observed over one full rotation. Here we assumed the nucleus to have a $\cos^{3/2}\theta$ scattering law and a spin-axis perpendicular to the line of sight (see Section 3). From this fit (Fig. 2) we obtained a bandwidth estimate $B = 22.9 \pm 1.4$ Hz, where the error represents one standard deviation as determined from a Monte Carlo noise simulation. This bandwidth is nearly four times larger than that estimated from the 1980 Encke detection. It is also much larger than the bandwidths measured for the five other radar-detected comet nuclei, all of which had $B < 6$ Hz at $\lambda = 12.6$ cm (Harmon et al., 1999, 2004). This implies that Encke is relatively large and/or a fast rotator.

3. Bandwidth and spin axis

The total Doppler bandwidth B of a spherical rotating nucleus is

$$B = \frac{8\pi R \sin\alpha}{\lambda P}, \tag{1}$$

where R is the nucleus radius, P is the rotation period, and α is the angle between the spin axis and the Earth–comet line. For an aspherical nucleus, B depends on α and P as well as the nucleus shape and dimensions and the range of rotational phases spanned by the integration period (Jurgens, 1982). Although Encke's nucleus is believed to be significantly elongated, this cannot account for the large change in B between the two apparitions, as both the 1980 and 2003 observations spanned a wide range of rotational phase. Instead, we consider it most likely that the dominant contributor to the bandwidth difference is the change in aspect angle α associated with the different observing geometries. This is plausible given the large difference in the geocentric coordinates of the comet between the two apparitions. These coordinates are listed in Table 2 and the aspect geometry is shown

Table 2
Encke spin-axis aspect

Date (UT)	R.A. (°)[a]	Dec. (°)[a]	α (°)[b]
2003 November 23.8	289.1	18.1	91.1
2003 November 25.8	284.9	14.6	87.0
1980 November 02.6	192.5	34.3	34.6
1980 November 08.6	204.6	17.6	18.7

[a] Comet geocentric coordinates at tabulated date.
[b] Angle between the comet spin vector and the comet–Earth vector. The comet's pole direction is assumed to be (R.A. = 198°, Dec. = 0°) (Festou and Barale, 2000).

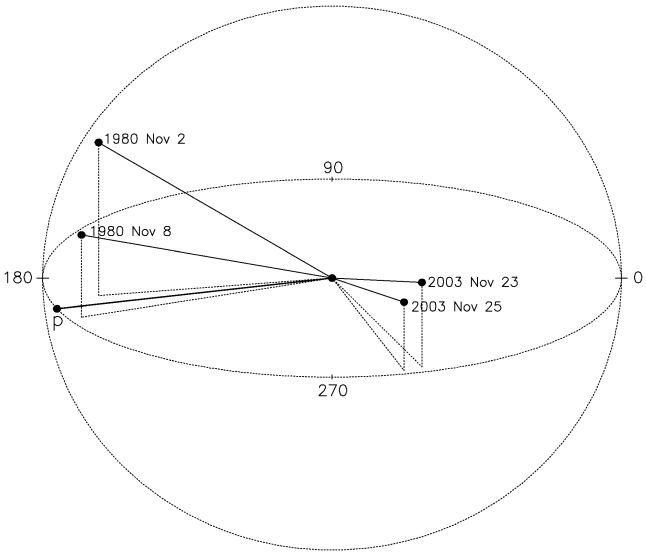

Fig. 4. Comet Encke positions, in geocentric equatorial coordinates, for the first and last dates of the 1980 and 2003 radar campaigns (see Table 2). Also shown is the spin-axis direction (p) used to compute the aspect angles in Table 2.

in Fig. 4. Sekanina (1988, 1991) proposed a spin-axis direction of 206° right ascension, +4° declination, based on a detailed study of the outgassing geometry over many apparitions; his uncertainty or "common-solution area" defined by the constraints from the various apparitions spans 8° in right ascension and 7° in declination. In a recent reanalysis of optical data from the 1980 apparition, Festou and Barale (2000) proposed a refined pole position of 198° right ascension, 0° declination, with a stated uncertainty of "a few degrees." Their pole direction is shown in Fig. 4. Using the Festou and Barale pole, we have calculated the range of α angles during the 1980 and 2003 radar campaigns (Table 2). Note that this assumed pole direction would have the spin-axis essentially perpendicular ($\alpha \approx 90°$) to the 2003 line of sight (see Fig. 4), giving the maximum possible Doppler spread. By contrast, the same spin axis would have been aimed more toward the Earth during the 1980 observations, the $\sin\alpha$ projection reducing the Doppler bandwidth by a factor of 1.8–3.1 between the November 2 start date and the November 8 end date, respectively. For comparison, the 2003 radar observations gave a bandwidth 3.8 times larger than the 6 Hz quoted for 1980. The difference (between the 3.8 and 1.8–3.1 factors) may not be significant, given the uncertainty in the 1980 bandwidth and the fact that the best 1980 observations going into the average spectrum were made during the second half of the campaign, when the spin axis was more closely aligned toward the Earth and the $1/\sin\alpha$ projection factor was closer to 3. It is possible, of course, that there is a modest error in the Festou–Barale pole direction and that the true spin axis was even more closely aligned with the 1980 line of sight than indicated by Table 2 and Fig. 4. Such would be the case if the true pole direction were to have a modest positive declination (see Fig. 4), which would be consistent with the constraints reported in Sekanina (1988).

An alternative, or contributing, explanation for the bandwidth difference is that there was some change in the spin vector between 1980 and 2003 associated with a shift or precession of the axis, a spin-up of the rotation, or both. A significant spin-axis shift seems unlikely given Encke's stable fan geometry (Sekanina, 1988), large size, and modest activity. There was, however, some evidence for a change in the primary periodicity of Encke's optical light curves from 15 h in the 1980's to 11 h in 2002 that suggested a change in rotation period. Some studies have suggested that the earlier 15-h periodicity was an artifact of cometary activity at aphelion rather than a true rotation period (Meech et al., 2001; Samarasinha et al., 2004; Belton et al., 2004a, 2004b), although Fernández et al. (2004a) did not discount the possibility that the 15-h period and implied spin-up were real. Nevertheless, while we cannot rule out the possibility of some contribution from spin-up, it is clear than most of the radar bandwidth increase between 1980 and 2003 can simply be attributed to the change in observing aspect relative to a stable spin axis close to that specified by Sekanina (1988) and Festou and Barale (2000).

4. Rotation, size, and radar albedo

Our CW observations, lacking any range resolution, do not provide us with a direct estimate of nucleus size. Furthermore, as noted in Section 2, our data are not suitable for inferring a rotation period from changes in the spectrum shape and bandwidth. What we do have is a reasonably accurate estimate of $B = 22.9$ Hz for the maximum Doppler bandwidth of the nucleus. Also, arguments given in Section 3 suggest that we can set $\sin\alpha = 1$ with reasonable confidence. Then, assuming the oblong nucleus to be in principal-axis (PA) rotation about the short axis (see caveats below), we can rewrite Eq. (1) to give a size-to-period ratio

$$\frac{a\ (\mathrm{km})}{P\ (\mathrm{h})} = 0.412, \tag{2}$$

where a is the semimajor axis. Using this ratio as a constraint, as shown in Fig. 5, we can then evaluate the plausibility of various combinations of size and period that have been proposed on the basis of independent (i.e., nonradar) observations.

Published rotation period estimates for Encke span a wide range between 6 and 22 h (Whipple and Sekanina, 1979; Jewitt and Meech, 1987; Luu and Jewitt, 1990; Sekanina, 1991; Samarasinha et al., 2004; Fernández et al., 2002, 2004a, 2004b). This corresponds to long-axis lengths of 5–18 km (Fig. 5). Recently, evidence has been found for a dominant 11.0–11.1 h light-curve periodicity that may be indicative of a dominant rotation with that same period (Fernández et al., 2002, 2004a, 2004b; Lowry et al., 2003; Christian et al., 2004). This corresponds to a long-axis dimension of ~9 km for a PA rotator (Fig. 5). However, there

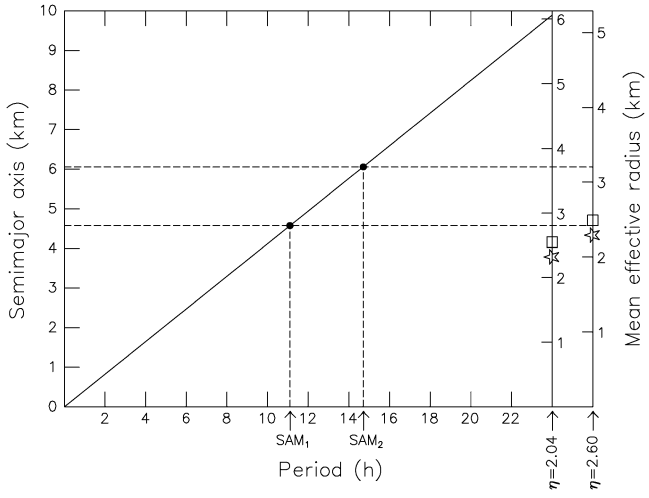

Fig. 5. Nucleus semimajor axis vs rotation period (solid line) based on the measured radar Doppler bandwidth and Eq. (2). The right-hand scales give the corresponding mean effective radius for a prolate spheroidal nucleus with axial ratio $\eta = 2.04$ and $\eta = 2.60$ and assuming observation from an $\alpha = 90°$ aspect. The radar-based sizes for two different SAM solutions ($P = 11.1$ h and $P = 14.7$ h) are delineated (dashed lines). Also shown are the R_{eff} values estimated by Campins (1988) (squares) and Fernández et al. (2000) (stars). The error in the Fernández et al. (2000) sizes is ±0.3 km.

is enough complexity in the light curves to suggest that Encke's nucleus is in an excited rotation state (Samarasinha et al., 2004; Belton et al., 2004a, 2004b; Fernández et al., 2004a). Belton et al. argue that one could still maintain the observed sunward coma fan if the nucleus were in a moderately excited, short-axis-mode (SAM) rotation state in which the dominant motion is a high-angle precession (with period P_ϕ) of the long axis about the total angular momentum vector. In addition, there would be an oscillation about the long axis with period P_ψ and a rocking or nutation of the long axis with period $P_\theta = P_\psi$. The analysis of Belton et al. (2004a, 2004b) shows that Encke's rotation is equally well described by two different low-energy SAM states. We will refer to these two possible states as: SAM_1, with $P_\phi = 11.1$ h, $P_\psi = 47.6$ h; and SAM_2, with $P_\phi = 14.7$ h, $P_\psi = 46.6$ h. With either model solution, the P_θ nutation is a rocking of only a few degrees about $\theta = 90°$. Furthermore, for a prolate spheroidal nucleus the P_ψ oscillation would not contribute to the maximum bandwidth. Hence, Eq. (2) should still give a close approximation to the a/P ratio if one sets $P = P_\phi$. Accordingly, we have used this equation to plot lines in Fig. 5 corresponding to the dominant periodicities $P = 11.1$ h and $P = 14.7$ h from the two SAM solutions in the Belton et al. model. This gives $a \approx 4.6$ km for SAM_1 and $a \approx 6.1$ km for SAM_2 (see also Table 3). (Note that for a cylindrical, rather than spheroidal, nucleus the P_ψ oscillation would contribute about 5% to the maximum bandwidth, in which case a would be overestimated by the same amount.)

We can check the plausibility of, or distinguish between, the two SAM solutions by comparing their corresponding size estimates with sizes based on infrared (IR) observations. The IR-based sizes are expressed in terms of a mean effective radius $R_{\rm eff} = \sqrt{A/\pi}$, where A is the estimated mean projected area of the nucleus during the observations. Therefore, we have included $R_{\rm eff}$ scales on the right-hand side of Fig. 5. Here we take the nucleus to be a prolate spheroid with axial ratio $\eta = a/b$ (where b is the semiminor axis) and have averaged evenly over all rotational phases assuming $\alpha = 90°$. We plot two different $R_{\rm eff}$ scales corresponding to two different axial ratios: $\eta = 2.04$, which is the value favored by Belton et al. (2004a, 2004b) based on their reinterpretation of the IR data of Fernández et al. (2000); and $\eta = 2.60$, which is the original IR-based lower limit for η quoted by Fernández et al. (2000). The $R_{\rm eff}$ estimates inferred from combining the Belton et al. SAM solutions with the radar bandwidth are shown in Fig. 5 and listed in Table 3. Shown for comparison on Fig. 5 are the $R_{\rm eff}$ values reported from the IR observations of Campins (1988) and Fernández et al. (2000). Campins reported $R_{\rm eff} < 2.9$ km, the inequality representing an allowance for possible dust-coma contamination rather than a detection upper limit. Since Campins' observations were made at a nearly pole-on ($\alpha \sim 10°$) aspect, we have adjusted his $R_{\rm eff}$ value downwards by ≈0.4 km to correct it to our reference aspect angle of $\alpha = 90°$. The $R_{\rm eff} = 2.4 \pm 0.3$ km value of Fernández et al. required a much smaller downward adjustment given the fairly large pole angle ($\alpha \sim 65°$) during their observations.

Table 3
Nucleus size and radar albedo estimates

P (h)	a (km)	η	$R_{\rm eff}$ (km)	$\hat{\sigma}$
11.1	4.58	2.04	2.81	0.042
		2.60	2.42	0.055
14.7	6.06	2.04	3.72	0.024
		2.60	3.21	0.032

From Fig. 5 we can see that a comparison of radar bandwidth with IR-based sizes definitely favors the 11.1-h (SAM_1) rotation solution over the 14.7-h (SAM_2) rotation solution. (The 14.7-h solution gives an $R_{\rm eff}$ that differs from the Fernández et al. value by three times their quoted estimation error.) For the $\eta = 2.6$ case, the $a = 4.6$ km, $P = 11.1$ h combination gives a very close match to the radar and IR data. Whether one can use this comparison to argue strongly for $\eta > 2.04$ remains questionable, given the model dependence of the IR sizes and possible departures of the nucleus shape from a prolate spheroid. If, however, SAM_1 can be taken to be an accurate representation of Encke's spin state, then the radar estimate of 9.2 km should be an accurate estimate of the long-axis dimension. Note that if the nucleus is more cylindrical in shape, then the long axis would be slightly smaller (8.7 km).

From their analysis of Encke light curves from near-aphelion observations in 2001–2002, Fernández et al. (2004a) concluded the dominant synodic rotation period was either 11.08 h or its subharmonic of 22.16 h. Our results in Fig. 5 indicate that we can definitely rule out the 22-h period in favor of the 11-h period. This would also seem to invalidate the 22.4-h synodic period proposed by Jewitt and Meech (1987) from 1985 light curves, although these same authors suggested that the 11.2-h harmonic was also a possibility. The fast (6-h) rotation proposed by Whipple and Sekanina (1979) is also inconsistent with our results.

From the nucleus size estimates and radar cross section one can estimate the intrinsic radar reflectivity of the nucleus. This is expressed in terms of a radar albedo $\hat{\sigma}$ defined by

$$\hat{\sigma} = \frac{\sigma}{\pi R_{\rm eff}^2}, \tag{3}$$

where $\sigma = \sigma_{\rm oc} + \sigma_{\rm sc}$ is the total radar cross section. In Table 3 we list the $\hat{\sigma}$ values obtained using the $\sigma = 1.02$ km^2 value from the 3-day average spectrum (Table 1) and the $R_{\rm eff}$ values from the various spin/shape models. Note that for the preferred 11-h rotation period one gets $\hat{\sigma} \sim 0.05$. This is not far from the $\hat{\sigma} = 0.039$ estimate for Comet C/IRAS–Araki–Alcock, which had been considered the most reliable comet radar albedo estimate up to this time (Harmon et al., 1989, 1999, 2004). The new Encke albedo estimate provides strong support for the earlier conclusion (Harmon et al., 1999, 2004) that comet radar albedos are comparatively low (∼0.05), typically less than half that of near-Earth and

mainbelt asteroids (Ostro et al., 1991; Magri et al., 2001; Harmon et al., 2004; L.A.M. Benner, personal comm.). Following arguments given in Harmon et al. (1999, 2004), the Encke albedo indicates a nucleus surface density of 0.5–1.0 g cm^{-3}, which would correspond to a dense terrestrial snowpack or a powdery soil. (This density would apply to surface layers down to the penetration depth of the radar wave, which is of the order of 20 wavelengths for 1 g cm^{-3} soils.) Although nucleus surfaces and interiors do not necessarily have the same structure, it is interesting to note that our inferred surface density range is similar to most current estimates of the overall bulk density of comet nuclei (e.g., Weissman et al., 2004). Furthermore, while the radar observations of Encke and other comets indicate that comet surfaces are loosely compacted, they do not support the extremely low-density (<0.2 g cm^{-3}) or "fractal" models that are sometimes proposed (e.g., Hughes, 1996).

5. Grain-coma nondetection

Encke is the parent of the Taurid meteor stream (Klačka and Pittich, 1998) and also the source of a narrow infrared dust trail (Sykes et al., 1986; Reach et al., 2000), so it is likely to be producing the sort of large (>cm) grains that would be detectable with radar. Given this association with meteoroids, and the fact that short-period comets such as Encke are suspected to play an important role in the interplanetary dust budget, any radar-derived estimate of the large-grain production rate would be of interest. Based on observations during the 1977 apparition, Sekanina and Schuster (1978) concluded that Encke's large-grain production was insignificant compared to that needed to replenish the interplanetary dust population. Fulle (1990), using the same 1977 data but a different model, derived grain production rates for Encke that were considerably higher than Sekanina and Schuster's. Fulle's higher production rates have since been supported by the modeling work of Epifani et al. (2001) based on 1997 observations. Based on these estimates, we had concluded in our preobservation planning that there was a good chance of detecting a large-grain coma echo similar to that seen from several other comets. Hence, the fact that we saw no hint of grains is an interesting result that warrants further discussion.

We start by making a rough estimate of an upper limit for Encke's coma-echo cross section based on a comparison with two comets for which we did obtain coma detections. In Fig. 3b we show the 100-Hz-smoothed coma echoes for Comets C/IRAS–Araki–Alcock and C/2001 A2 (LINEAR). Comparing the amplitudes of these coma echoes with the 3-standard-deviation level of the undulations in the smoothed Encke spectrum, we conclude that any Encke coma echo must have had less than 14% of the amplitude of the C/2001 A2 coma echo and less than 39% of the amplitude of the C/IRAS–Araki–Alcock coma echo. Using the measured coma cross sections for these two comets (Harmon et al., 1989, 2004; Nolan et al., 2004), we get an upper limit (3 standard deviation) for the radar cross section of Encke's grain coma of 0.3 or 0.6 km^2, depending on whether the coma echo is narrower (like IRAS–Araki–Alcock) or wider (like C/2001 A2).

Using this cross section upper limit we compute the corresponding upper limit for $\dot{M}(a_\mathrm{m})$, which is the total particulate mass loss rate as a function of the maximum grain radius a_m. We calculated $\dot{M}(a_\mathrm{m})$ using Eq. (B9) of Harmon et al. (1989), which also appears as Eq. (24) of Harmon et al. (2004). We assumed that the grains are dirtballs of density $\rho = 1$ g cm^{-3} and that the grain size distribution followed an $a^{-3.5}$ power-law size distribution. Then, assuming $\sigma < 0.45$ km^2 (a compromise between the two limits given above), we calculated an $\dot{M}(a_\mathrm{m})$ upper-limit curve that is well approximated by

$$\dot{M}(a_\mathrm{m}) < \begin{cases} 2\times10^4\ \mathrm{g\,s^{-1}} & (a_\mathrm{m} > 2\ \mathrm{cm}), \\ 2\times10^4 (a_\mathrm{m}/2\ \mathrm{cm})^{-3}\ \mathrm{g\,s^{-1}} & (a_\mathrm{m} < 2\ \mathrm{cm}), \end{cases} \quad (4)$$

where the break at $a_\mathrm{m} = 2$ cm corresponds to the transition between small grains in the Rayleigh scattering regime ($a_\mathrm{m} < \lambda/2\pi$) and larger grains in the Mie scattering regime. Since this estimate assumes a constant production rate, but includes grains ejected as much as a month or so earlier (when the true production rate should have been lower), it probably underestimates the instantaneous production rate by about a factor of two. Even so, the radar upper limit for the $a_\mathrm{m} > 2$ cm case is still about 5 times smaller than the $\sim 2\times10^5$ g s^{-1} production rates estimated by Fulle (1990) and Epifani et al. (2001) from optical/infrared data at this same preperihelion distance and assuming the same 1 g cm^{-3} grain density. It is also significantly less than the 1.4×10^5 g s^{-1} estimated by Lisse et al. (2004) from 1997 postperihelion observations at a solar distance of 1.17 AU. In other words, had Encke been producing large grains at the rate predicted by optical/infrared modeling of earlier (1977 and 1997) apparitions, we should have detected them.

Why then, did we not detect a coma echo? One possibility is that the grains were disintegrating or evaporating before they had a chance to fill an appreciable portion of the radar beam. However, the optical/infrared models are based on nondisintegrating grains fanning out over comparably large distances. Furthermore, Encke's grain emission must include a substantial population of long-lived refractory grains, as these are the ones that must be surviving long enough to form the infrared trail (Reach et al., 2000); in fact, Reach (2004) has argued that Encke's mass loss from refractory grains exceeds by several times the mass loss from evaporating ices. Another possibility is that the largest grains were actually smaller than the Rayleigh–Mie transition scale ($a = \lambda/2\pi \sim 2$ cm) at the time of the radar observations. This is not unreasonable given that (1) Comet C/IRAS–Araki–Alcock showed an apparent size cutoff of a few centimeters (Harmon et al., 1989, 1999, 2004), and (2) Encke's gas production (and, possibly, its corresponding grain lifting capacity) was less than that of IRAS–Araki–

Alcock. This, however, conflicts with the assertion of Fulle (1990) and Epifani et al. (2001) that a_m should be of the order of a decimeter at this preperihelion epoch, when Encke's large-grain production should be near its peak. Furthermore, Reach et al. (2000) argue that the grains making up the core of Encke's infrared dust trail should have radii in excess of 5 cm. A third possibility is that the large grains are fluffier than is implied by the assumed $\rho = 1\ \mathrm{g\,cm^{-3}}$ density. Invoking fluffier grains would raise the radar upper limit for $\dot{M}$, since increasing the grain porosity lowers the backscatter per unit mass. It would presumably also lower the infrared $\dot{M}$ estimates, since the absorption per unit mass (or opacity) increases with porosity. This same argument has also been suggested as a way to reconcile $\dot{M}$ values derived from radar coma echoes with those derived from radio continuum observations (Harmon et al., 1997, 2004). Also, fractal grains have been suggested as a possible explanation for the low optical scattering albedo of Encke's extended dust tail (Lisse et al., 2004). Finally, there is the possibility that, for some reason, Encke's preperihelion grain production was lower than normal during its last apparition. Preliminary IR data from the Spitzer Space Telescope do, in fact, suggest that Encke's 2003 preperihelion dust and large-grain production was low (Reach, 2004). It should of course be pointed out, by way of a cautionary note, that it is very difficult to make reliable comparisons between dust-grain models based on entirely different types of observations and using different sets of assumptions and simplifications. Hence, our conclusions regarding the grain coma are subject to much more uncertainty than are our inferences about the inherently much simpler nucleus echo.

6. Conclusion

The 2003 apparition of Comet Encke gave us our first opportunity to get a second look at a comet with radar. Comparison of the new radar results with the 1980 radar detection and with nonradar observations has enabled us to place strong constraints on the size, rotation, and surface density of the Encke nucleus. Unfortunately, Encke does not make a comparably close approach to us for at least the next forty years, and the closest approach in the near future (October, 2013) only gets to within 0.48 AU. Hence, barring dramatic improvements in radar systems, it is unlikely there will be any significant new radar results for this comet before the eventual reconnaissance by an imaging spacecraft. In the meantime, continued ground-based and Earth-orbital observations in the optical and infrared may result in further refinement in our knowledge of Encke's size, shape, rotation, and grain production. This may, in turn, allow additional comparisons to be made with the existing radar data on this comet. Ultimately, of course, a definitive determination of Encke's properties must await a spacecraft encounter.

Acknowledgments

We thank Jon Giorgini (JPL/Caltech) for providing the observing ephemeris. Michael Belton kindly read an early draft and offered helpful suggestions pertaining to Encke's rotation state and its significance for the radar interpretation. These observations were made possible by technical support from transmitter engineers Joe Greene, Victor Negrón, and Jon Hagen. The National Astronomy and Ionosphere Center (Arecibo Observatory) is operated by Cornell University under a cooperative agreement with the National Science Foundation and with support from the National Aeronautics and Space Administration.

References

Belton, M., Samarasinha, N., Fernández, Y., Meech, K., 2004a. The excited spin state of Comet 2P/Encke. COSPAR Scientific Assembly 35th. Abstract COSPAR-A-01483.

Belton, M.J.S., Samarasinha, N.H., Fernández, Y.R., Meech, K.J., 2004b. The excited spin state of Comet 2P/Encke. Icarus. In press.

Campins, H., 1988. The anomalous dust production in periodic Comet Encke. Icarus 73, 508–515.

Christian, D.J., Lisse, C.M., Dennerl, K., Wolk, S.J., Bodewits, D., Combi, M.R., Hoekstra, R., Makinen, J.T.T., Weaver, H.A., 2004. Chandra observations of a collisionally and optically thin charge exchange system Comet 2P/Encke 2003. Bull. Am. Astron. Soc. 36, 1117.

Epifani, E., Colangeli, L., Fulle, M., Brucato, J.R., Bussoletti, E., De Sanctis, M.C., Mennella, V., Palomba, E., Palumbo, P., Rotundi, A., 2001. ISOCAM imaging of Comets 103P/Hartley 2 and 2P/Encke. Icarus 149, 339–350.

Fernández, Y.R., Lowry, S.C., Weissman, P.R., Meech, K.J., 2002. New dominant periodicity in photometry of Comet Encke. Bull. Am. Astron. Soc. 34, 887.

Fernández, Y.R., Lisse, C.M., Käufl, H.U., Peschke, S.B., Weaver, H.A., A'Hearn, M.F., Lamy, P.P., Livengood, T.A., Kostiuk, T., 2000. Physical properties of the nucleus of Comet 2P/Encke. Icarus 147, 145–160.

Fernández, Y.R., Lowry, S.C., Weissman, P.R., Mueller, B.E.A., Samarasinha, N.H., Belton, M.J.S., Meech, K.J., 2004a. New near-aphelion light curves of Comet 2P/Encke. Icarus. In press.

Fernández, Y.R., Lisse, C.M., Schleicher, D.G., Bus, S.J., Kassis, M., Hora, J.L., Deutsch, L.K., 2004b. The nucleus of Comet 2P/Encke as observed in the fall 2003 apparition. Bull. Am. Astron. Soc. 36, 1117.

Festou, M.C., Barale, O., 2000. The asymmetric coma of comets. I. Asymmetric outgassing from the nucleus of Comet 2P/Encke. Astron. J. 119, 3119–3132.

Fulle, M., 1990. Meteoroids from short period comets. Astron. Astrophys. 230, 220–1226.

Harmon, J.K., Campbell, D.B., Ostro, S.J., Nolan, M.C., 1999. Radar observations of comets. Planet. Space Sci. 47, 1409–1422.

Harmon, J.K., Campbell, D.B., Hine, A.A., Shapiro, I.I., Marsden, B.G., 1989. Radar observations of Comet IRAS–Araki–Alcock 1983d. Astrophys. J. 338, 1071–1093.

Harmon, J.K., Ostro, S.J., Benner, L.A.M., Rosema, K.D., Jurgens, R.F., Winkler, R., Yeomans, D.K., Choate, D., Cormier, R., Giorgini, J.D., Mitchell, D.L., Chodas, P.W., Rose, R., Kelley, D., Slade, M.A., Thomas, M.L., 1997. Radar detection of the nucleus and coma of Comet Hyakutake (C/1996 B2). Science 278, 1921–1924.

Harmon, J.K., Nolan, M.C., Ostro, S.J., Campbell, D.B., 2004. Radar studies of comet nuclei and grain comae. In: Festou, M., et al. (Eds.), Comets II. Univ. of Arizona Press, Tucson. In press.

Hughes, D.W., 1996. The interior of a cometary nucleus. Planet. Space Sci. 44, 705–710.

Jewitt, D., Meech, K., 1987. CCD photometry of Comet P/Encke. Astron. J. 93, 1542–1548.

Jurgens, R.F., 1982. Radar backscatter from a rough rotating triaxial ellipsoid with applications to the geodesy of small asteroids. Icarus 49, 97–108.

Kamoun, P.G.D., 1983. Radar observations of cometary nuclei. PhD thesis, Massachusetts Institute of Technology, Cambridge.

Kamoun, P.G., Pettengill, G.H., Shapiro, I.I., 1982a. Radar detectability of comets. In: Wilkening, L.L. (Ed.), Comets. Univ. of Arizona Press, Tucson, pp. 288–296.

Kamoun, P.G., Campbell, D.B., Ostro, S.J., Pettengill, G.H., Shapiro, I.I., 1982b. Comet Encke: radar detection of nucleus. Science 216, 293–295.

Klačka, J., Pittich, E.M., 1998. Origin of the Taurid meteor stream. Planet. Space Sci. 46, 881–886.

Lisse, C.M., Fernández, Y.R., A'Hearn, M.F., Grün, E., Käufl, H.U., Osip, D.J., Lien, D.J., Kostiuk, T., Peschke, S.B., Walker, R.G., 2004. A tale of two very different comets: ISO and MSX measurements of dust emission from 126P/IRAS (1996) and 2P/Encke (1997). Icarus 171, 444–462.

Lowry, S.C., Weissman, P.R., Sykes, M.V., Reach, W.T., 2003. Observations of periodic Comet 2P/Encke: physical properties of the nucleus and first visual-wavelength detection of its dust trail. Lunar Planet. Sci. 34. Abstract 2056.

Luu, J., Jewitt, D., 1990. The nucleus of Comet P/Encke. Icarus 86, 69–81.

Magri, C., Consolmagno, G.J., Ostro, S.J., Benner, L.A.M., Beeney, B.R., 2001. Radar constraints on asteroid regolith properties using 433 Eros as ground truth. Meteorit. Planet. Sci. 36, 1697–1709.

Meech, K.J., Fernández, Y., Pittichová, J., 2001. Aphelion activity of 2P/Encke. Bull. Am. Astron. Soc. 33, 1075.

Nolan, M.C., Harmon, J.K., Howell, E.S., Campbell, D.B., Margot, J.-L., 2004. Detection of large grains in the coma of Comet C/2001 A2 (LINEAR) from Arecibo radar observations. Icarus. Submitted for publication.

Ostro, S.J., Campbell, D.B., Chandler, J.F., Hine, A.A., Hudson, R.S., Rosema, K.D., Shapiro, I.I., 1991. Asteroid 1986 DA: radar evidence for a metallic composition. Science 252, 1399–1404.

Ostro, S.J., Hudson, R.S., Benner, L.A.M., Giorgini, J.D., Magri, C., Margot, J.-L., Nolan, M.C., 2002. Asteroid radar astronomy. In: Festou, M., et al. (Eds.), Asteroids III. Univ. of Arizona Press, Tucson, pp. 151–168.

Reach, W.T., 2004. Infrared observations of comets with the Spitzer Space Telescope. Bull. Am. Astron. Soc. 36, 1174.

Reach, W.T., Sykes, M.V., Lien, D., Davies, J.K., 2000. The formation of Encke meteoroids and dust trail. Icarus 148, 80–94.

Samarasinha, N.H., Mueller, B.E.A., Belton, M.J.S., Jorda, L., 2004. Rotation of cometary nuclei. In: Festou, M., et al. (Eds.), Comets II. Univ. of Arizona Press, Tucson. In press.

Sekanina, Z., 1988. Outgassing asymmetry of periodic Comet Encke: I. Apparitions 1924–1984. Astron. J. 95, 911–924.

Sekanina, Z., 1991. Encke, the comet. J. Roy. Astron. Soc. Can. 85, 324–376.

Sekanina, Z., Schuster, H.E., 1978. Dust from periodic Comet Encke: large grains in short supply. Astron. Astrophys. 68, 429–435.

Sykes, M.V., Lebofsky, L.A., Hunten, D.M., Low, F., 1986. The discovery of dust trails in the orbits of periodic comets. Science 232, 1115–1117.

Weissman, P.R., Asphaug, E., Lowry, S.C., 2004. Structure and density of cometary nuclei. In: Festou, M., et al. (Eds.), Comets II. Univ. of Arizona Press, Tucson. In press.

Whipple, F.L., Sekanina, Z., 1979. Comet Encke. Precession of the spin axis, nongravitational motion, and sublimation. Astron. J. 84, 1894–1909.

Yeomans, D.K., Chodas, P.W., Keesey, M.S., Ostro, S.J., Chandler, J.F., Shapiro, I.I., 1992. Asteroid and comet orbits using radar data. Astron. J. 103, 303–317.